

## Supplementary information

### Summary of trace element partitioning regression procedure

The crystal structure of amphibole includes several crystallographic sites with different coordination and size that can accommodate a range of trace elements, including large ion lithophile elements (Rb, Sr, Ba), Pb, U, Th, high field strength elements (Ti, Zr, Hf, Nb and Ta), rare earth elements (REE) and Y, and transitional metals (e.g. Tiepolo et al. 2007). Elements with large ionic radius (e.g. Rb, Pb) are accommodated in the A site, while highly charged high-field strength elements (e.g.  $\text{Zr}^{4+}$ ) substitute for Ti on the M2 site (Oberti *et al.*, 2000), and REE and Y partition onto the M4 site (Brenan et al. 1995; Klein et al. 1997; Hilyard et al. 2000; Shimizu et al. 2017). To account for the strong crystal-chemical control on partitioning, we used multiple regression (MR) methods to predict amphibole-melt trace element partition coefficients from the major element composition of the crystal, using a compilation of 13 published high-temperature experimental studies. These studies covered a wide range of conditions (200-2,500 MPa, 780-1,100 °C) and melt compositions (basanite to rhyolite) and crystallised calcic amphiboles (pargasite – edenite – hastingsite – magnesiohastingsite – kaersutite – tschermakite – magnesiohornblende). Temperature was not included as an independent variable. Amphibole formula components were used as independent variables, including  $\text{Si}_T$ ;  $\text{Al}_{VI}$ ; M1-3 site Ti,  $\text{Fe}^{3+}$ , and  $\text{Fe}^{2+}$ ;  $\text{Ca}_{M4}$ ; and  $\text{Na}_A$ . We calculated the ‘average  $\text{Fe}^{3+}$ ’ stoichiometry following Leake et al. (1997). See Humphreys et al. (in review) for further details. For major elements, we used a revised form of the major element regression scheme of Zhang et al. (2017).

### References

- Tiepolo, M., Oberti, R. & Zanetti, A. (2007) Trace-element partitioning between amphibole and silicate melt. *Reviews in Mineralogy and Geochemistry* 67, 417–452
- Oberti, R., Vannucci, R., Zanetti, A., Tiepolo, M. & Brumm, R.C. (2000) A crystal chemical re-evaluation of amphibole/melt and amphibole/clinopyroxene  $D_{Ti}$  values in petrogenetic studies. *American Mineralogist*, 85, 407-419
- Brenan J.M., Shaw H.F., Ryerson F.J. & Phinney D.L. (1995) Experimental determination of trace-element partitioning between pargasite and a synthetic hydrous andesitic melt. *Earth and Planetary Science Letters* 135, 1–11
- Klein, M., Stosch, H.-G., Seck, H.A. (1997) Partitioning of high field-strength and rare-earth elements between amphibole and quartz-dioritic to tonalitic melts: an experimental study. *Chemical Geology* 138, 257–271
- Hilyard, M., Nielsen, R.L., Beard, J.S. et al (2000) Experimental determination of the partitioning behaviour of rare earth and high field strength elements between pargasitic amphibole and natural silicate melts. *Geochimica et Cosmochimica Acta* 64, 1103–1120
- Shimizu, K., Liang, Y., Sun, C., Jackson, C.R.M. & Saal, A.E. (2017) Parameterized lattice strain models for REE partitioning between amphibole and silicate melt. *American Mineralogist* 102, 2254–2267
- Leake, B.E., Woolley, A.R., Arps, C.E.S., et al (1997) Nomenclature of amphiboles: report of the subcommittee on amphiboles of the International Mineralogical Association, Commission on New Minerals and Mineral Names. *Canadian Mineralogist* 35, 219–246
- Humphreys, M.C.S., Cooper, G.F., Zhang, J., Loewen, M., Kent, A.J.R., Macpherson, C.G. & Davidson, J.P. (in review) Amphibole reveals the hidden complexity of lower crustal magma plumbing systems at arcs. *Contributions to Mineralogy and Petrology* (in review)

**Regression equations used to calculate major element amphibole equilibrium melts (AEM), after Zhang et al. (2017); Zhang et al. (erratum).** An example is given below the table. The parameter “lnSiPoly” is equivalent to a polynomial of the tetrahedral Si content:

$$\ln\text{SiPoly} = -164.73 \cdot \ln\text{Si}_T^2 + 757.99 \cdot \ln\text{Si}_T - 772.44$$

Results of multiple linear regressions used for estimating melt major element compositions on the basis of temperature and calcic-amphibole component. N = 130

Eq.	Dependent variable	Parameters used	Range of variation	Constant	Si	lnSiPoly	Al (vi)	Mg	Fe3+	Fe2+	Ti	Ca	Na (A)	Multiple R <sup>2</sup>	SE (wt %)	se (wt%)
1	SiO <sub>2</sub> (wt %)	lnSiPoly	39.6 - 79.2	-138.2109 ± 25.3058		1.5533 ± 0.1298	19.9584 ± 4.4996		30.2722 ± 4.4616	7.3331 ± 0.8076	44.9836 ± 9.1473	36.5966 ± 7.4745		0.839	3.73	5.31
4	lnTiO <sub>2</sub>	Si <sub>T</sub>	-2.8 - 1.8	19.1540 ± 1.16484	-2.7852 ± 0.16672			1.0678 ± 0.07654	-1.6996 ± 0.19083			-2.2233 ± 0.49808	-1.6150 ± 0.41673	0.825	0.64	0.39
7	lnFeO	Si <sub>T</sub> , Fe <sub>T</sub>	-0.34 - 2.75	16.5023 ± 1.1184	-2.1604 ± 0.1261			0.2928 ± 0.0734				-1.4158 ± 0.4284		0.705	2.18	2.71
8	lnMgO	Si <sub>T</sub>	-2.19 - 2.47	12.9140 ± 0.93019	-2.6555 ± 0.14592		1.0045 ± 0.27452	1.2374 ± 0.07951						0.800	1.12	1.28
9	lnCaO	Si <sub>T</sub> , Fe <sub>T</sub>	-2.19 - 2.47	6.2200 ± 0.61322	-1.1514 ± 0.09619		1.2727 ± 0.18097	0.6931 ± 0.05241						0.708	1.45	1.94
10	K <sub>2</sub> O (wt %)	Si <sub>T</sub>	<6.0	31.6434 ± 5.4085	-2.6611 ± 0.6548		-6.4625 ± 0.8317	-1.3486 ± 0.1607	-5.0597 ± 0.7102		-6.1714 ± 1.3617		-5.7344 ± 0.9997	0.586	0.76	0.91
11	Al <sub>2</sub> O <sub>3</sub>	Si <sub>T</sub>	11.4 - 21.5	29.8766 ± 4.1070	-2.5551 ± 0.5681		2.9594 ± 0.8313						4.8840 ± 1.2277	0.530	1.31	1.45

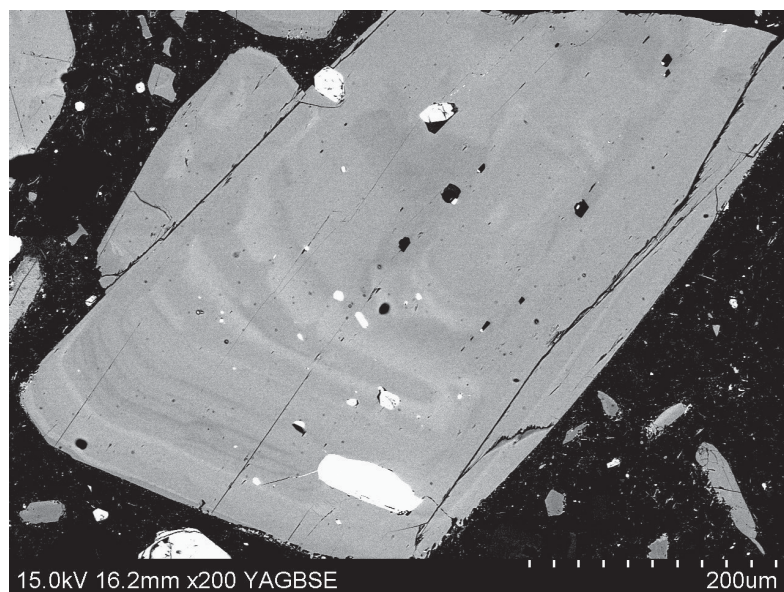
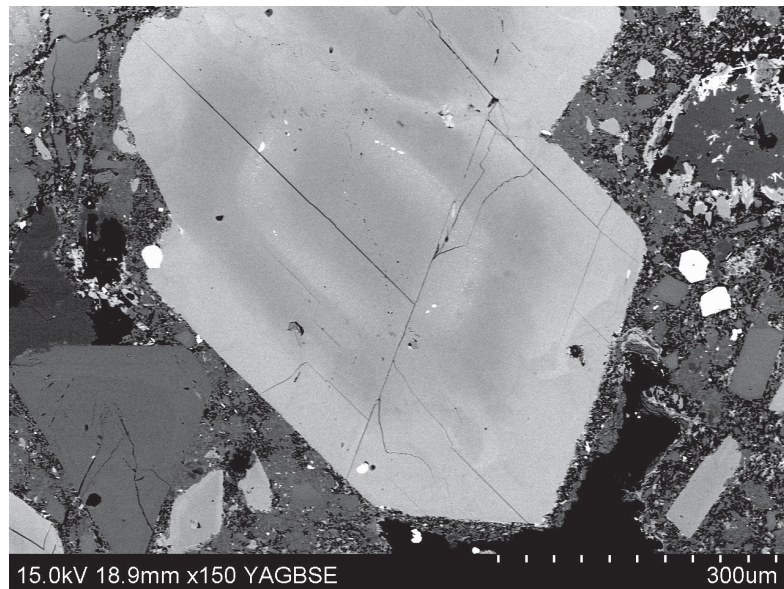
Normal font indicates p-value < 0.01; bold font indicates the p-value of the parameter or the constant is 0.01 ≤ p-value < 0.05

e.g.  $\ln\text{TiO}_2 \text{ (wt\%)} = 19.1540 - 2.7852 \cdot \text{Si} + 1.0678 \cdot \text{Mg} - 1.6996 \cdot \text{Fe}^{3+} - 2.2233 \cdot \text{Ca} - 1.6150 \cdot \text{Na}_A$

**Regression equations used to calculate trace element amphibole equilibrium melts (AEM), after Humphreys et al. (in review). An example is given below the table.**

	Intercept	Si	Al <sub>IV</sub>	Ti	Fe <sup>3+</sup>	Fe <sup>2+</sup>	Ca	NaA	SE	R <sup>2</sup>
lnDRb	9.1868	-1.3898		-3.6797	-1.5769	-0.6938			0.286	0.85
±	2.4481	0.3989		0.629	0.4764	0.16				
lnDSr	3.41585	-0.75281				0.36529			0.191	0.64
±	0.84461	0.13988				0.05751				
lnDPb	-4.2533		2.7155	1.69	0.7065			-1.0433	0.226	0.57
±	0.3242		0.364	0.433	0.2733			0.395		
lnDU	5.2962			-2.3538			-5.1786		0.557	0.53
±	1.6004			0.7793			0.8921			
lnDNb	-22.27	2.3241		3.7633	2.9786	1.44	1.8719		0.446	0.6
±	3.8207	0.4364		0.8944	0.5331	0.1552	0.751			
lnDZr	-25.6167	2.6183	2.6867	4.838	2.6591	0.6536	2.5248		0.489	0.46
±	6.2797	0.646	0.8747	1.4983	0.7124	0.1496	0.927			
lnDLa	-20.0493	2.0732		2.5498	1.5317	1.117	2.2771	-1.4576	0.338	0.69
±	2.7427	0.3151		0.6107	0.2794	0.1325	0.5098	0.4684		
lnDCe	-21.1078	2.4749		2.4719	1.5722	0.952	1.5311		0.316	0.82
±	2.747	0.3122		0.7001	0.2899	0.1451	0.4978			
lnDNd	-20.3082	2.5162		2.5863	1.9459	0.9566	1.2763		0.362	0.71
±	2.869	0.3125		0.7628	0.2911	0.1264	0.5252			
lnDSm	-11.3625	1.602			1.2898	1.2376			0.426	0.6
±	0.614	0.1046			0.29	0.1218				
lnDEu	-35.6604	4.1452	2.6886	6.4057	3.8508	0.7255	3.0679		0.372	0.77
±	7.2875	0.7354	1.0276	1.6219	0.7596	0.1546	1.1127			
lnDGd	-19.0583	2.4417		1.9786	1.8765	0.9943	1.3677		0.403	0.66
±	3.5099	0.3715		0.8105	0.3785	0.1607	0.6517			
lnDDy	-16.0687	2.3858		1.8255	1.9741	0.6922			0.333	0.79
±	1.1469	0.1721		0.4663	0.2559	0.1077				
lnDHo	-20.4148	2.3654		2.484	3.2601	1.2922	3.1762	-4.9224	0.398	0.84
±	4.9365	0.5324		1.3325	0.6081	0.4288	1.1052	1.0816		
lnDYb	-15.8659	2.281		1.5905	2.1534	0.7867			0.426	0.66
±	1.4239	0.2228		0.5474	0.3275	0.1684				
lnDLu	-19.3462	2.1142		2.8478	2.7011	1.0402	2.9625	-3.2356	0.395	0.74
±	3.3662	0.3998		0.8937	0.6972	0.2336	0.9835	0.876		
lnDY	-36.2514	3.6078	3.78	7.513	4.8366	0.814	4.6048		0.323	0.71
±	7.9576	0.9806	1.0445	1.6764	0.7101	0.1737	0.7871			

e.g.  $\ln D_{La} = -20.0493 + 2.0732 \cdot Si + 2.5498 \cdot Ti + 1.5317 \cdot Fe^{3+} + 1.117 \cdot Fe^{2+} + 2.2771 \cdot Ca - 1.4576 \cdot Na_A$



Supplementary figure S1.

Representative back-scattered electron images illustrating “diffuse-zoned” (top, from LAM-14) and “spiky-zoned” (bottom, from LAM-23) oscillatory zoning, showing multiple excursions to high Mg-number.